

OpenREAD: Reinforced Open-Ended Reasoning for End-to-End Autonomous Driving with LLM-as-Critic

Songyan Zhang^{1*}, Wenhui Huang^{2*}, Zhan Chen¹,
Chua Jiahao Collister¹, Qihang Huang¹, Chen Lv^{1†}

¹ Nanyang Technological University, Singapore ² Harvard University, USA

<https://github.com/wyddmw/OpenREAD>

Abstract

Recently, two-stage fine-tuning strategies, e.g., acquiring essential driving knowledge through supervised fine-tuning (SFT) and further enhancing decision-making and planning via reinforcement fine-tuning (RFT), have shown strong potential in advancing the knowledge-driven autonomous driving (AD) paradigm. However, the learning nature of SFT still limits the generalization of reasoning, thereby constraining the full potential of driving performance. Meanwhile, current RFT approaches are primarily applied to downstream tasks, since scene understanding is an open-ended problem where corresponding rewards are difficult to quantify. To address these limitations, we propose OpenREAD, an **OPEN**-ended **R**einforced **E**nd-to-**E**nd **A**utonomous **D**riving (**AD**) framework that enables end-to-end RFT across the full spectrum from high-level reasoning to low-level trajectory planning. Specifically, we begin by constructing large-scale Chain-of-Thought (CoT) annotations on open-source driving-related knowledge datasets, and employ the powerful Qwen3 large language model (LLM) as the critic in RFT to quantify reasoning quality for open-ended questions during reward modeling. Extensive experiments confirm that joint end-to-end RFT yields substantial improvements in both upstream and downstream tasks, enabling OpenREAD to achieve state-of-the-art performance on reasoning and planning benchmarks.

1. Introduction

Autonomous driving has witnessed remarkable progress in recent years, largely propelled by breakthroughs in machine learning algorithms such as convolutional neural networks [14, 36], and transformers [35, 52]. This progress has been further promoted by the rapid growth of large-scale, high-quality datasets [4, 10, 12, 49], tailored for the

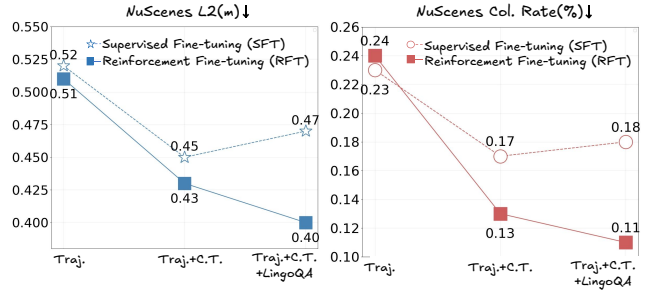


Figure 1. **Comparison between RFT and SFT with increased driving-related knowledge.** Traj. denotes the data of trajectory planning only, and C.T. denotes the data of counterfactual trajectory analysis. Extending driving knowledge through RFT leads to a notable improvement on the NuScenes dataset compared with SFT.

development of individual modules—including perception, prediction, and planning, etc. More recently, end-to-end (E2E) data-driven paradigms have been proposed to integrate these traditionally independent components into a unified framework [7, 17, 23, 31, 59]. Such E2E data-driven approaches enable the joint optimization across perception, prediction, and planning modules, facilitating scalability in both model parameters and training data, and obtaining substantial performance improvements. However, as discussed in [28], contemporary methods still face significant challenges, including overfitting to training data, limited generalization to long-tail and cross-domain scenarios, and the lack of interpretability. For instance, a stop sign displayed on an advertisement screen may mislead autonomous vehicles into abnormal driving behaviors, highlighting a key limitation of purely data-driven approaches that focus on direct input–output mapping without knowledge induction and causal reasoning.

The emergence of generalized human-like intelligence in recent advances of Large Language Models (LLMs) [5,

62, 63] and Vision-Language Models (VLMs) [2, 8, 9, 27, 34, 57, 64] offers a promising bridge to leverage extensive knowledge for addressing the aforementioned challenges. Pioneering studies have explored replacing traditional end-to-end models with VLM-based architectures, taking advantage of their reasoning and linguistic capabilities to enable knowledge-driven autonomous driving [19, 20, 46, 48, 51, 56, 67]. However, most existing approaches adopt a supervised fine-tuning (SFT) paradigm and rely heavily on fixed answer patterns, which limits their flexibility and generalization in linguistic representation and semantic diversity. Inspired by the success of reinforcement fine-tuning (RFT) [41], particularly the recent advances in DeepSeek-R1 [13], Group Relative Policy Optimization (GRPO) [47] has been introduced in several early studies [24, 30, 72] to strengthen reasoning ability. Nevertheless, these works primarily focus on verifiable tasks such as meta-decision making [24] or trajectory planning [30, 72], where outputs are deterministic and easily quantifiable. In contrast, real-world autonomous driving involves numerous open-ended reasoning tasks. For example, in response to the question “*Why are you decelerating?*”, multiple contextually reasonable answers may exist. This reveals an important and underexplored challenge: *How can we effectively integrate open-ended driving knowledge with concrete driving behaviors to extend reasoning and driving performance beyond fixed ground-truth supervision?*

To tackle this challenge, we propose OpenREAD, an **OPEN**-ended **R**easoning reinforced vision-language model (VLM) designed for autonomous driving (**AD**). OpenREAD handles a broad spectrum of tasks, ranging from open-ended reasoning such as perception and scene understanding to verifiable driving behaviors such as trajectory planning. This capability is achieved through a joint end-to-end RFT paradigm over both open-ended knowledge and planning datasets, enhancing generalization and reasoning capabilities while improving downstream planning performance. Inspired by the training protocol of DeepSeek-R1 [13], we begin with cold-start initialization. GPT-4 [1] is employed to generate reasoning annotations on a subset of LingoQA [40], a large-scale open-ended driving knowledge dataset covering scenario perception and action-related tasks. We further incorporate the OmniDrive dataset [54] by converting its annotations into reasoning-based textual trajectories. After equipping the model with foundational driving knowledge through supervised fine-tuning (SFT), we perform end-to-end RFT using GRPO [47] to further enhance reasoning quality. For open-ended questions without explicit ground truth, Qwen3-8B serves as a critic to assess the generated responses with continuous rewards. In addition, rewards based on semantic similarity and average displacement error (ADE) are introduced to encourage the model to learn to reason and drive rather than merely imitating ground-truth

answers or behaviors.

Extensive experiments demonstrate that joint end-to-end RFT substantially improves both upstream reasoning and downstream planning, enabling OpenREAD to achieve state-of-the-art performance on reasoning and planning benchmarks. Our main contributions are summarized as follows:

1. We present a thinking-enabled autonomous driving model that employs RFT across both knowledge learning and trajectory planning, extending the end-to-end learning paradigm beyond traditional SFT.
2. We introduce an LLM-as-critic mechanism that allows GRPO to be applied not only to verifiable tasks but also to open-ended knowledge learning, making end-to-end RL feasible for autonomous driving.
3. We construct a set of Chain-of-Thought (CoT) datasets designed to equip autonomous driving models with essential domain knowledge and explicit reasoning capability.

2. Related Works

2.1. End-to-End Autonomous Driving

End-to-end autonomous driving abandons the traditional pipeline of separate perception, prediction and planning modules in favor of a single learning-based framework that maps raw sensor inputs directly to motion plans or control actions [29, 60]. Such approaches have recently gained traction thanks to large-scale driving datasets, improved simulation tools and deep learning methods for joint feature optimization [6, 7, 17, 21]. DriveTransformer [22] unifies perception, prediction, and planning within a single Transformer architecture, enabling direct cross-task and sensor-to-task attention for efficient and scalable end-to-end driving. ParaDrive [59] emphasizes the interdependence of sub-tasks and proposes a parallelized structure to improve coordination between prediction and planning. DiffusionDrive [33] introduces a generative diffusion model that produces diverse and continuous trajectory candidates, enhancing motion diversity under uncertain conditions. Despite these advances, existing end-to-end methods still fall short in capturing high-level scene semantics and complex agent interactions, which limits their ability to generalize to diverse, long-tail, or previously unseen driving scenarios [25].

2.2. LLMs and VLMs for Autonomous Driving

The recent rise of LLMs and VLMs has sparked growing interest in bringing semantic reasoning and general world knowledge into autonomous driving. Early explorations such as ADAPT [26], DriveGPT4[61] and LMDrive [46] adapt VLMs for tasks like scene captioning, reasoning, or language-guided control, demonstrating the feasibility of integrating linguistic priors into autonomous driving. Subsequent systems like DriveVLM [51], DriveMLM [56], RAG-Driver [66], and ELM [70] expanded this direction by in-

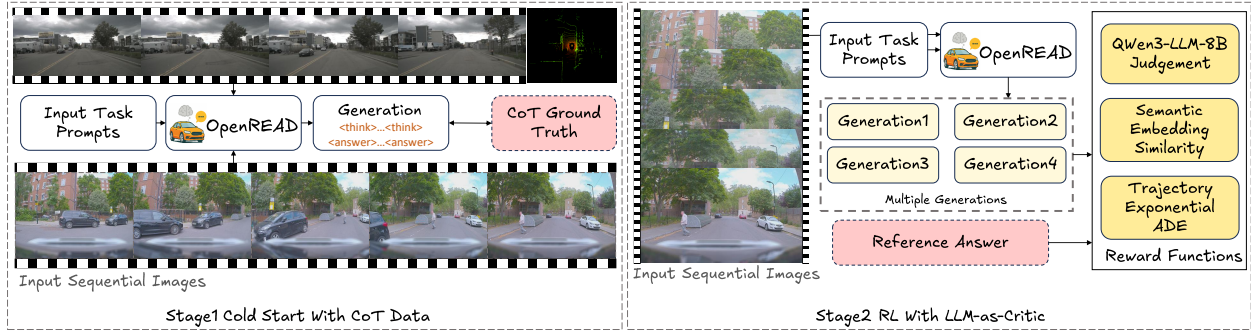


Figure 2. The training pipeline of our OpenREAD. For the cold start stage, we utilize the CoT annotated data for SFT, followed by RFT with GRPO to further enhance the reasoning capabilities.

corporating multi-modal perception or retrieval-augmented knowledge, but most models either rely solely on supervised fine-tuning or provide only high-level decisions without producing actionable trajectories.

More recent work has begun leveraging VLMs for deeper semantic reasoning that directly supports motion-related predictions [58, 71]. SimLingo [44] aligns natural-language instructions with driving actions by combining VLM-based language understanding, instruction-conditioned policy learning, and closed-loop trajectory generation from camera-only input. ORION [11] integrates long-context visual encoding with an LLM-based reasoning module to enrich scenario interpretation before generating trajectories. OpenDriveVLA [69] proposes a language-driven supervision and evaluation pipeline, demonstrating the feasibility of text-conditioned motion assessment. AutoVLA [72] introduces autoregressive action modeling within a VLM backbone and shows that structured reasoning signals can benefit downstream planning under reinforcement fine-tuning. ReCog-Drive [30] adopts a cognition-to-planning pipeline where VQA-aligned language features condition a diffusion-based motion predictor. On the data side, OmniDrive [54] provides large-scale video QA and counterfactual reasoning annotations built on nuScenes [4], supplying strong supervision for causal and semantic understanding.

2.3. Reinforcement Fine-Tuning for LLMs and VLMs

RFT has recently emerged as an effective paradigm for improving the reasoning capability of LLMs and VLMs. Methods such as Vision Think [65] and Visual RFT [37] extend RFT to visual or multimodal settings, allowing models to refine intermediate reasoning steps under verifiable rewards. Vision-R1 [18] further adapts the DeepSeek-R1 paradigm [13] to vision-based tasks, showing that stepwise reward-driven optimization can significantly enhance visual logical reasoning. Reason-RFT [50] generalizes this idea to broader multimodal problems by coupling structured reason-

ing traces with reward-based updates, improving consistency and factuality. These works collectively demonstrate that reward-driven reasoning optimization can substantially improve the semantic understanding and decision quality of large models. In autonomous driving, where both open-ended scene reasoning and motion-related predictions require multi-step inference, such reinforcement tuning strategies offer a promising mechanism for jointly enhancing high-level reasoning and downstream decision-making.

3. Methodology

3.1. Overview of OpenREAD

Our OpenREAD is built on top of the Qwen3-VL-8B model [64]. The overall framework and training pipeline is illustrated in Fig. 2. Given a sequence of images along with the task-specific textual prompts as input, our OpenREAD is capable of generating the corresponding answers with an explicit thinking process. Specifically, we use five sequential images of the front view for open-ended driving knowledge learning and four sequential images along with a Lidar Bird-Eye’s View image of the current timestep for the trajectory planning task, as inspired by [19, 43, 56] to integrate the surrounding 3D information. The fine-tuning process involves two stages: cold start with the CoT annotated data in a SFT, followed by the RFT with GRPO algorithm. We will give a detailed description of each stage in the following sections.

3.2. Cold Start

3.2.1. CoT Data Generation

To endow the model with fundamental reasoning and thinking capabilities, we start with CoT annotations for cold start. Specifically, we adopt the LingoQA dataset [40] as our primary source of driving-related knowledge, which provides high-quality question-answer pairs covering both scenario understanding and action analysis tasks. We manually annotate 100 samples with concise rationales that focus key objects within each scenario, avoiding redundant reasoning

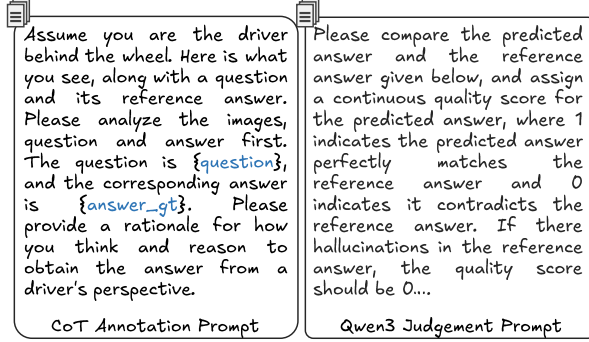


Figure 3. An overview of the prompt templates used for CoT annotation generations (Left) and Qwen3-LLM open-ended driving knowledge evaluation (Right).

contents. These annotated examples are subsequently provided to GPT-4.1 to summarize the target annotation prompt, as illustrated in the left panel of Fig. 8.

We then leverage the derived annotation prompt and provide GPT-4.1 with the corresponding images, questions, and reference answers to generate target rationales from a driver’s perspective. The placeholder of $\{question\}$ and $\{answer_gt\}$ will be updated accordingly during the generation process. After manually post-processing to refine or discard inappropriate outputs, we obtain a total of 7K high-quality CoT annotations for driving knowledge on the LingoQA dataset, as in Fig. 4.

Moreover, we incorporate the OmniDrive dataset, a well-annotated CoT dataset built on the NuScenes dataset. We separate the original mixture of reasoning and answer contents, and reformat the data into our target structure by enclosing the reasoning within $<think>...</think>$ and the ground-truth answers within $<answer>...</answer>$. The modified OmniDrive dataset integrates two tasks: trajectory planning and counterfactual trajectory analysis. Representative examples are illustrated in Fig. 4. For the trajectory planning task, the reasoning component describes the high-level meta action and its underlying rationale, while the answer provides a future trajectory of six points over the next three seconds at 2 Hz. For the counterfactual trajectory analysis task, a pseudo trajectory is given, and the objective is to determine whether this trajectory is reasonable. This task helps the model to have a more comprehensive understanding of the planning and improves the spatial perception capabilities of the surroundings. The total amount of CoT annotations for the trajectory planning and counterfactual trajectory analysis tasks is 24K and 7K, respectively.

3.2.2. SFT with CoT Data

Given a sequence of N images $X_v \in \mathbb{R}^{N \times H \times W \times 3}$, a set of visual tokens $H_v \in \mathbb{R}^{N_v \times D_v}$ is obtained from the vision encoder and the projector, where N_v and D_v denote the vi-

sual token number and the feature dimension for each image, respectively. Conditioned on the textual instruction X_t and its corresponding textual embeddings H_t , the LLM computes the probability of the target answer Y_a in autoregression:

$$p(Y_a | H_v, H_t) = \prod_{i=1}^L p(y_i | H_v, H_t, y < i), \quad (1)$$

where L is the length of the target answer. The cross-entropy function is then applied to compute the loss between the prediction and ground-truth.

3.3. RFT with LLM-as-Critic

3.3.1. Preliminary on GRPO Algorithm

To further enhance the reasoning capability of OpenREAD, we introduce a second RFT stage based on the GRPO algorithm [47]. In contrast to traditional reinforcement learning methods such as Proximal Policy Optimization (PPO) [45], which rely on a critic network for policy evaluation, GRPO simplifies the reward mechanism by directly comparing groups of candidate responses. Given a query q that integrates the visual input and task-specific instruction, GRPO samples a set of outputs o_1, o_2, \dots, o_G from the previous policy $\pi_{\theta_{\text{old}}}$ and computes the normalized group-relative advantage A_i :

$$A_i = \frac{r_i - \text{mean}(\{r_j\}_{j=1}^G)}{\text{std}(\{r_j\}_{j=1}^G)}, \quad (2)$$

where r_i is the reward value for the i -th sample. The current policy π_{θ} is then optimized by maximizing the objective:

$$\mathcal{J}_{\text{GRPO}}(\theta) = \mathbb{E}_{q, \{o_i\} \sim \pi_{\theta_{\text{old}}}} \left[\frac{1}{G} \sum_{i=1}^G (\mathcal{J}_i^R - \beta \mathbb{D}_{\text{KL}}(\pi_{\theta} \| \pi_{\text{ref}})) \right], \quad (3)$$

$$\mathcal{J}_i^R = \min(w_i A_i, \text{clip}(w_i, 1 - \epsilon, 1 + \epsilon) A_i), \quad (4)$$

where $w_i = \frac{\pi_{\theta}(o_i | q)}{\pi_{\theta_{\text{old}}}(o_i | q)}$, and ϵ and β are hyper-parameters.

3.3.2. Open-ended Knowledge Rewards

A key component of the RFT stage lies in the design of the reward function, which guides the model to efficiently explore and optimize its policy. To address the challenge of open-ended knowledge rewards assignment discussed before, we employ Qwen3-LLM [63] as an automatic evaluator that functions as a classifier to assign reward scores. The key components of the user prompt are illustrated in the right panel of Fig. 8. The *predicted_answer* and *reference_answer* are updated accordingly during the training process. For each predicted response and its reference answer, Qwen3-LLM outputs a continuous value between 0 and 1 representing the probability that the predicted answer semantically matches the reference. This value is then discretized based on a

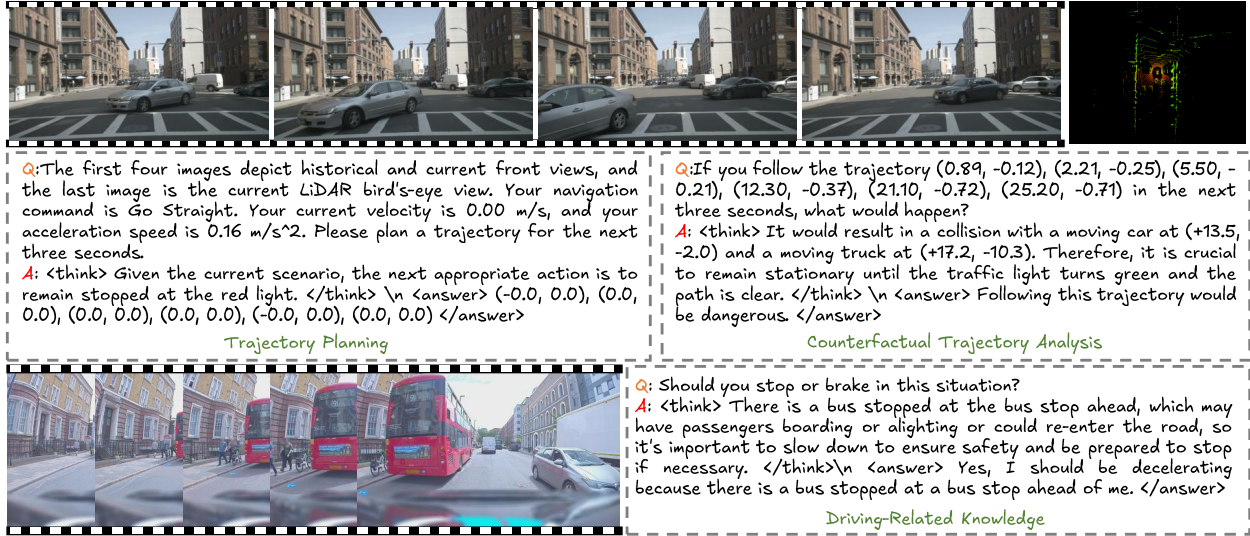


Figure 4. An overview of our CoT annotations for driving-related knowledge and trajectory planning.

predefined threshold, which is 0.5 in this work. The Qwen3-LLM reward R_{qwen3} for the i -th predicted response r_{q_i} is:

$$r_{q_i} = \begin{cases} 1, & \text{if } p_i > 0.5, \\ 0, & \text{else,} \end{cases} \quad (5)$$

where p_i denotes the probability assigned by Qwen3-LLM to the i -th predicted response.

To further encourage the model to omit the redundant reasoning and produce concise outputs, we introduce an additional semantic-level reward, R_{semantic} . This reward is computed by extracting the sentence embeddings of both the predicted response and the reference answer by [55]¹, followed by calculating their cosine similarity, which ranges from 0 to 1. A higher similarity score indicates that the predicted response exhibits a closer alignment in expression, including sentence length, semantic meaning, and overall phrasing.

The overall reward for open-ended knowledge learning R_{know} is a weighted combination of the Qwen3-LLM reward R_{qwen3} and the semantic embedding similarity R_{semantic} :

$$R_{\text{know}} = w_q R_{\text{qwen3}} + w_s R_{\text{semantic}}, \quad (6)$$

where w_q and w_s are weighting hyperparameters set to 0.9 and 0.1, respectively.

3.3.3. Trajectory Planning Reward

Given the i -th sample of the planned trajectory and the ground truth over the next 3 seconds at 2Hz (resulting in 6 points in total), we compute the average L_2 distance for each

second, denoted as $\{d_{i1}, d_{i2}, d_{i3}\}$. The trajectory reward R_{traj} for the current sample r_{traj_i} is then calculated as:

$$r_{t_i} = 5^{-d_{i1} * T_1} + e^{-d_{i2} * T_2} + e^{-d_{i3} * T_3}, \quad (7)$$

where T_n is the temperature scalar for the n -th second. In our work, the temperatures are set to 0.7, 0.7, 0.3 for corresponding 1s, 2s, and 3s.

3.3.4. Joint Training

During the RFT stage, the trajectory planning task is jointly trained with the learning of driving-related knowledge. The default format reward R_{format} is also adopted to constrain the reasoning components enclosed in $<\text{think}> \dots </\text{think}>$ and the final response enclosed in $<\text{answer}> \dots </\text{answer}>$. The overall reward is a combination of R_{know} and R_{traj} for the corresponding responses within a batch:

$$R = R_{\text{know}} + R_{\text{traj}} + R_{\text{format}}. \quad (8)$$

4. Experiment

4.1. Implementation Details

We leverage the training framework of Model-Swift [68], an official framework provided by the ModelScope community for fine-tuning and deploying large language models and multi-modal large models. Our OpenREAD is implemented on top of the Qwen3-VLM-8B [64] dense model. For the cold-start stage, we conduct supervised fine-tuning with a total batch size of 32 on 4 NVIDIA-H100 GPUs. The learning rate is set to 1×10^{-4} with a warm-up ratio of 0.05, followed by a cosine decay schedule. It takes one epoch of fine-tuning on the CoT-annotated datasets introduced in

¹We use a finetuned version of <https://huggingface.co/microsoft/Minilm-L12-H384-uncased>.

Table 1. Effectiveness of extending driving-related knowledge via RFT for both trajectory planning and knowledge learning. Jointly learning trajectory planning and driving-related knowledge with enhanced reasoning capabilities through RFT substantially reduces the L2 distance error and improves knowledge acquisition, outperforming the SFT notably.

Data	Epoch	Type	Traj Eval								Know Eval	
			L2 (m) ↓			Collision (%) ↓				Coun.	Traj.↑	LingoQA↑
			1s	2s	3s	Avg.	1s	2s	3s	Avg.	GPT-Score	LingoJudge
Traj.	1	SFT	0.22	0.48	0.85	0.52	0.06	0.14	0.50	0.23	-	-
	1	Cold-Start	0.22	0.48	0.84	0.51	0.09	0.13	0.43	0.22	-	-
	1	RFT	0.23	0.48	0.83	0.51	0.05	0.18	0.49	0.24	-	-
Traj.+Count.Traj.	1	SFT	0.20	0.43	0.73	0.45	0.05	0.10	0.37	0.17	62.2%	-
	1	Cold-Start	0.21	0.44	0.74	0.46	0.03	0.11	0.36	0.17	67.0%	-
	1	RFT	0.20	0.42	0.68	0.43	0.03	0.07	0.30	0.13	67.4%	-
Traj.+Count.Traj. +LingoQA	1	SFT	0.20	0.44	0.76	0.47	0.06	0.11	0.37	0.18	65.6%	66.4%
	2	SFT	0.20	0.42	0.71	0.44	0.03	0.07	0.29	0.13	68.0%	67.4%
	1	Cold-Start	0.19	0.41	0.71	0.44	0.04	0.10	0.30	0.15	68.2%	65.4%
	1	RFT	0.18	0.37	0.63	0.40	0.04	0.07	0.20	0.11	68.8%	68.2%

Sec. 3.2.1, which include driving-related knowledge and trajectory planning on the LingoQA, [40], and OmniDrive [54] datasets. The training data amounts for the cold start stage are 7K, 9K, and 24K for LingoQA, counterfactual trajectory analysis, and trajectory planning, respectively.

The RFT stage is initialized from the cold start checkpoint. To maintain a balanced learning ratio between trajectory planning and driving-related reasoning, we randomly sample 6K trajectory planning examples and 5K mixed samples from LingoQA and counterfactual trajectory data. For each training step, the number of response generations is set to 4. The learning rate is set to 1×10^{-4} with a total batch size of 16. We employ LoRA [15] and utilize the AdamW [38] optimizer during both the SFT and RFT stages.

4.2. Evaluation Metric

For driving-related knowledge evaluation, we report the official Lingo-Judge metric for the LingoQA dataset which uses a pretrained text transformer to assess the semantic correctness of the predicted answer with respect to the question and reference response. We also report a GPT-score for evaluating the counterfactual trajectory analysis, which computes the average accuracy by utilizing the GPT-4.1 to evaluate whether the predicted response matches the reference. In addition, we follow previous works [34, 40, 70] and report three established metrics of CIDEr [53], BLEU [42], and Meteor [3] which collectively measure the similarity between generated explanations and reference descriptions, covering content relevance, n-gram consistency, and semantic matching. For the trajectory planning task on the NuScenes dataset, we report the ST-P3 [16] based metric in terms of the L2 distance error and collision rate across 1s, 2s, and 3s.

4.3. RFT for Knowledge-Enhanced Planning

We conduct thorough ablation experiments to assess the effectiveness of RFT and the necessity of extending driving-related knowledge. The results are presented in Tab. 1. When training on the trajectory-planning-only task, we use the full training set during the SFT and cold-start stages for one epoch. The RFT stage involves a set of 6K randomly sampled data. Due to the absence of driving-related knowledge data and relatively weak capabilities obtained at the cold-start stage, the subsequent RFT stage fails to deliver notable gains. In fact, the average collision rate even degrades at the 2-second and 3-second prediction. A similar degradation is also observed in AutoVLA [72]. These ablation studies indicate that performing RFT solely on trajectory planning provides only limited benefits, highlighting the necessity of extending driving-related knowledge.

To help the model achieve a more comprehensive understanding of the planning task, we further introduce the counterfactual trajectory analysis data. At this stage, we use the full set of trajectory planning data together with 9K counterfactual trajectory samples during the SFT and cold-start stages. During the RFT stage, we sample 6K trajectory-planning examples and 5K counterfactual trajectory analysis samples to achieve a balanced learning of planning ability and driving-related knowledge. The L2 distance and collision rate exhibit a significant improvement across the SFT, cold start, and RFT stages, strongly demonstrating the necessity of extending driving-related knowledge. It is worth noting that, when initialized from a well-established cold-start stage, the RFT training mechanism begins to exhibit a stronger potential at this stage. It outperforms the SFT by reducing the L2 distance from 0.45m to 0.43m and collision rate from 0.17% to 0.13%, respectively, demonstrating the effectiveness of knowledge extension via RFT in enhancing planning quality.

Table 2. Comparison of the Open-loop planning in nuScene. The ST-P3 evaluation protocol is used by default. \dagger : The ego status and planning trajectory are both processed by LLM in textual modality. \ddagger : Use a customized evaluation protocol instead of ST-P3 metrics.

Method	VLM-Based	Ego Status		L2 (m) \downarrow				Collision (%) \downarrow			
		BEV	Planner	1s	2s	3s	Avg.	1s	2s	3s	Avg.
VAD [23]	-	✓	✓	0.17	0.34	0.60	0.37	0.07	0.10	0.24	0.14
UniAD [17]	-	✓	✓	0.44	0.67	0.96	0.69	0.04	0.08	0.23	0.12
Ego-MLP [32]	-	✓	✓	0.46	0.76	1.12	0.78	0.21	0.35	0.58	0.38
OpenDrive-VLA \dagger [69]	✓	✓	-	0.15	0.31	0.55	0.33	0.01	0.08	0.21	0.10
ORION[11] \ddagger	✓	✓	✓	0.17	0.31	0.55	0.34	0.05	0.25	0.80	0.37
ST-P3 [16]	-	-	-	1.33	2.11	2.90	2.11	0.23	0.62	1.27	0.71
RoboTron-Drive \dagger, \ddagger [19]	✓	-	-	0.14	0.30	0.57	0.33	0.03	0.12	0.63	0.26
EMMA \dagger [20]	✓	-	-	0.14	0.29	0.54	0.32	-	-	-	-
OpenEMMA \dagger [20]	✓	-	-	1.45	3.21	3.76	2.81	-	-	-	-
DriveVLM \dagger [51]	✓	-	-	0.18	0.34	0.68	0.40	0.10	0.22	0.45	0.27
GPT-Drive \dagger [39]	✓	-	-	0.20	0.40	0.70	0.44	0.04	0.12	0.36	0.17
OmniDrive [54] \ddagger	✓	-	-	0.40	0.80	1.32	0.84	0.04	0.46	2.32	0.94
AutoVLA \dagger [72]	✓	-	-	0.25	0.46	0.73	0.48	0.07	0.07	0.26	0.13
OpenREAD (Ours) \dagger	✓	-	-	0.18	0.37	0.63	0.40	0.04	0.07	0.20	0.11

The introduction of the additional LingoQA dataset further extends the diversity of the driving knowledge, covering scene understanding and action analysis across a wide range of scenarios. The comprehensive questions about the object recognition, action justification, driving attention, *etc.*, help to improve the model with enhanced general perception and reasoning capabilities. The SFT training stage is performed on additional 10k LingoQA samples, while the CoT training stage uses 7K LingoQA with CoT annotations instead. Equipped with the reasoning capabilities, our OpenREAD efficiently obtains a notable improvement during the cold-start stage, which is further improved during the RFT stage by jointly learning the driving knowledge and planning through GRPO, outperforming the SFT with two epochs of training by an obvious margin. Besides the trajectory planning performance, extending the driving-related knowledge with enhanced reasoning capabilities also improves the acquisition of the knowledge, which is reflected by the improved GPT-score for the counterfactual trajectory analysis at the cold start stage. For the LingoQA dataset, the Lingo-Judge accuracy is also increased via RFT, increasing from 65.4% to 68.2%.

The overall experiments on the NuScenes trajectory evaluation and knowledge evaluation highlight that empowering the model with accumulated driving-related knowledge and enhanced reasoning capability through GRPO-based RFT is key to achieving consistent improvements in planning performance and knowledge acquisition. This strongly validates the effectiveness of employing Qwen3-LLM as the judgment mechanism in our framework.

4.4. State-of-the-Art Benchmark

As shown in Tab. 2, we conduct a comparison with other SOTA approaches. Due to the leverage of extensive internal training data, EMMA[20] achieves the lowest L2 distance error, even outperforming the traditional end-to-end models by a notable margin. Compared with other VLM-based models trained on a comparable data scale, our OpenREAD obtains competitive performance and yields the lowest collision rate in the final two seconds. It is worth noting that the comparison with AutoVLA [72] which is also trained via RFT but exclusively on the trajectory planning data, our method achieves an obvious improvement, further highlighting the necessity of joint learning with driving-related knowledge. For driving-related knowledge evaluation, we benchmark OpenREAD against both generalist and specialist models. As reported in Tab. 3, only Qwen2.5-VL [2] is able to generate concise responses, whereas others tend to produce overly verbose outputs, leading to degraded evaluation metrics. Compared with specialist models trained on the LingoQA dataset, OpenREAD achieves the highest Lingo-Judge accuracy, demonstrating the effectiveness of reinforcing reasoning capabilities through RFT.

We omit comparison results for counterfactual trajectory analysis because generalist models are unable to correctly interpret coordinate-based inputs, while specialist models were not trained on this task, resulting in poor performance across all baselines.

Table 3. Comparison with generalist and specialist VLMs on the LingoQA. Our OpenREAD achieves the highest Lingo-Judge accuracy. Generalist models tend to produce redundant responses, which results in significantly degraded performance.

Method	Lingo-Judge	CIDEr	BLEU	Meteor
LLava-OV-7B [27]	54.2%	0.39	0.03	0.08
Qwen2.5-VL-7B [2]	62.6%	0.54	0.07	0.11
Qwen3-VL-4B [64]	37.0%	0.00	0.00	0.04
Qwen3-VL-8B [64]	51.4%	0.00	0.01	0.11
InternVL3-5-8B [57]	48.2%	0.14	0.02	0.12
OpenEMMA [20]	29.0%	0.07	0.02	0.11
WiseAD [67]	60.4%	0.68	0.20	0.19
RoboTron-Drive [19]	59.2%	0.65	0.14	0.19
ReCogDrive [30]	67.8%	0.69	0.13	0.21
OpenREAD (ours)	68.2%	0.74	0.15	0.20

4.5. Ablation Studies

4.5.1. Reward for Driving Knowledge Learning

To validate the effectiveness of our proposed reward design for driving-related knowledge learning, we conduct ablation experiments on a fixed set of 10K samples from the LingoQA dataset. Our 7K CoT annotated data are built upon this 10K samples. Our 7K CoT-annotated data are constructed from this subset. We first investigate RFT initialized from the vanilla Qwen3-VLM, as reported in the first four rows of Tab.4. Leveraging Qwen3-LLM as the only reward signal yields only marginal improvement, increasing the Lingo-Judge accuracy from 51.4% to 52.0%. This limited gain is largely due to the absence of constraints on response style: the generated outputs remain verbose and contain redundant descriptive content, similar to the vanilla Qwen3-VLM. Such redundancy is directly reflected in the degraded CIDEr, BLEU, and Meteor scores. Introducing the semantic embedding similarity reward can effectively alleviate the redundancy issue. However, embedding-based similarity primarily captures global sentence structure and often fails to discriminate key contradictions between reference answers and model predictions. For instance, the two sentences “*I should decelerate*” and “*I should accelerate*” yield a similarity score of 0.6. This ambiguity in reward assignment can degrade the reinforcement learning process, as evidenced by higher CIDEr, BLEU, and Meteor scores but a substantially lower Lingo-Judge accuracy. The weighted combination of these two rewards, as described in Sec. 3.3.2, leads to improved accuracy while preserving the concise and straightforward expression style of the reference answers. This balance is reflected by consistent improvements across all evaluation metrics. Nevertheless, due to the lack of explicit guidance on the thinking and reasoning process, the

Table 4. Ablation on the reward design and cold start for knowledge learning through GRPO.

Method	Type	Reward	Lingo-Judge↑	CIDEr↑	BLEU↑	Meteor↑
w/o Cold Start	RL	Base	-	51.4%	0.00	0.01
		Qwen3	52.0%	0.37	0.03	0.10
		Semantic	52.4%	0.65	0.13	0.19
(7K)	RL	Full	59.2%	0.67	0.13	0.20
		Base	-	65.0%	0.71	0.15
		Qwen3	66.4%	0.72	0.14	0.20
		Semantic	63.2%	0.66	0.15	0.20
		Full	66.0%	0.75	0.15	0.21

Table 5. Ablation on the data scale for knowledge learning on the LingoQA. Increasing the data amount introduces a constant improvement across different stages.

Method	Data	Lingo-Judge↑	CIDEr↑	BLEU↑	Meteor↑
SFT	10k	65.6%	0.765	0.149	0.206
	50k	68.0%	0.773	0.147	0.208
Cold Start	3k	63.0%	0.664	0.138	0.201
	7k	65.0%	0.705	0.153	0.203
GRPO	3k	66.0%	0.753	0.154	0.205
	5k	67.2%	0.739	0.165	0.201
	10k	68.4%	0.756	0.168	0.202

overall performance still falls short of expectations.

Following DeepSeek-R1 [13], we employ a cold start stage with explicit thinking guidance. Introducing the 7K CoT annotations with explicit reasoning steps effectively equips the model with fundamental reasoning capabilities, improving the Lingo-Judge accuracy from 51.4% to 65.0% while maintaining satisfactory expression quality. This highlights the critical role of the cold start stage. Subsequently, continuing RFT on the remaining 3K samples from a well-initialized checkpoint further facilitates the exploration process: using Qwen3-LLM as the judgment signal yields the best Lingo-Judge performance, and incorporating the weighted embedding similarity additionally helps constrain the overall expression style to better align with the reference answers, which is finally adopted in our work.

4.5.2. Data Scale for Knowledge Learning

As shown in Tab. 5, we explore the effectiveness of the training data amount for SFT, cold-start, and RFT. Clearly, increasing the amount of training data helps to obtain a constant gain across different training stages. Compared with SFT that requires 50K training data to improve the Lingo-Judge from 65.6% to 68.0%, our OpenREAD takes advantage of the GRPO algorithm to explore multiple responses within a rollout, increasing the Lingo-Judge accuracy from

65.0% to 68.4% with only another 10K data after the cold-start stage.

5. Conclusion and Limitations

In this work, we present OpenREAD, an open-ended reasoning reinforced VLM designed for joint knowledge learning and trajectory planning through RFT paradigm. By incorporating Qwen3-LLM as the critic in RL loop, our approach enables effective reinforcement of open-ended knowledge through GRPO, leading to SOTA performance in both trajectory planning and knowledge evaluation. Due to the computational cost associated with multiple generations from OpenREAD and Qwen3-LLM, the current scale of datasets used for RFT training remains limited. We will further scale up the knowledge data in future research.

References

- [1] Josh Achiam, Steven Adler, Sandhini Agarwal, Lama Ahmad, Ilge Akkaya, Florencia Leoni Aleman, Diogo Almeida, Janko Altenschmidt, Sam Altman, Shyamal Anadkat, et al. Gpt-4 technical report. *arXiv preprint arXiv:2303.08774*, 2023. [2](#)
- [2] Shuai Bai, Keqin Chen, Xuejing Liu, Jialin Wang, Wenbin Ge, Sibo Song, Kai Dang, Peng Wang, Shijie Wang, Jun Tang, et al. Qwen2. 5-vl technical report. *arXiv preprint arXiv:2502.13923*, 2025. [2](#), [7](#), [8](#)
- [3] Satanjeev Banerjee and Alon Lavie. Meteor: An automatic metric for mt evaluation with improved correlation with human judgments. In *Proceedings of the acl workshop on intrinsic and extrinsic evaluation measures for machine translation and/or summarization*, pages 65–72, 2005. [6](#)
- [4] Holger Caesar, Varun Bankiti, Alex H Lang, Sourabh Vora, Venice Erin Liang, Qiang Xu, Anush Krishnan, Yu Pan, Giacarlo Baldan, and Oscar Beijbom. nuscenes: A multimodal dataset for autonomous driving. In *Proc. IEEE Conf. Comp. Vis. Patt. Recogn.*, pages 11621–11631, 2020. [1](#), [3](#)
- [5] Zheng Cai, Maosong Cao, Haojong Chen, Kai Chen, Keyu Chen, Xin Chen, Xun Chen, Zehui Chen, Zhi Chen, Pei Chu, Xiaoyi Dong, Haodong Duan, Qi Fan, Zhaoye Fei, Yang Gao, Jiaye Ge, Chenya Gu, Yuzhe Gu, Tao Gui, Aijia Guo, Qipeng Guo, Conghui He, Yingfan Hu, Ting Huang, Tao Jiang, Penglong Jiao, Zhenjiang Jin, Zhikai Lei, Jiaxing Li, Jingwen Li, Linyang Li, Shuaibin Li, Wei Li, Yining Li, Hongwei Liu, Jiangning Liu, Jiawei Hong, Kaiwen Liu, Kuikun Liu, Xiaoran Liu, Chengqi Lv, Haijun Lv, Kai Lv, Li Ma, Runyuan Ma, Zerun Ma, Wenchang Ning, Linke Ouyang, Jiantao Qiu, Yuan Qu, Fukai Shang, Yunfan Shao, Demin Song, Zifan Song, Zhihao Sui, Peng Sun, Yu Sun, Huanze Tang, Bin Wang, Guoteng Wang, Jiaqi Wang, Jiayu Wang, Rui Wang, Yudong Wang, Ziyi Wang, Xingjian Wei, Qizhen Weng, Fan Wu, Yingtong Xiong, Chao Xu, Ruiliang Xu, Hang Yan, Yirong Yan, Xiaogui Yang, Haochen Ye, Huaiyuan Ying, Jia Yu, Jing Yu, Yuhang Zang, Chuyu Zhang, Li Zhang, Pan Zhang, Peng Zhang, Ruijie Zhang, Shuo Zhang, Songyang Zhang, Wenjian Zhang, Wenwei Zhang, Xingcheng Zhang, Xinyue Zhang, Hui Zhao, Qian Zhao, Xiaomeng Zhao, Fengzhe Zhou, Zaida Zhou, Jingming Zhuo, Yicheng Zou, Xipeng Qiu, Yu Qiao, and Dahua Lin. Internlm2 technical report, 2024. [1](#)
- [6] Li Chen, Penghao Wu, Kashyap Chitta, Bernhard Jaeger, Andreas Geiger, and Hongyang Li. End-to-end autonomous driving: Challenges and frontiers. *IEEE Trans. Pattern Anal. Mach. Intell.*, 2024. [2](#)
- [7] Shaoyu Chen, Bo Jiang, Hao Gao, Bencheng Liao, Qing Xu, Qian Zhang, Chang Huang, Wenyu Liu, and Xinggang Wang. Vadv2: End-to-end vectorized autonomous driving via probabilistic planning. *arXiv preprint arXiv:2402.13243*, 2024. [1](#), [2](#)
- [8] Zhe Chen, Jiannan Wu, Wenhui Wang, Weijie Su, Guo Chen, Sen Xing, Muyan Zhong, Qinglong Zhang, Xizhou Zhu, Lewei Lu, et al. Internvl: Scaling up vision foundation models and aligning for generic visual-linguistic tasks. In *Proc. IEEE Conf. Comp. Vis. Patt. Recogn.*, pages 24185–24198, 2024. [2](#)
- [9] Xiangxiang Chu, Limeng Qiao, Xinyu Zhang, Shuang Xu, Fei Wei, Yang Yang, Xiaofei Sun, Yiming Hu, Xinyang Lin, Bo Zhang, et al. Mobilevlm v2: Faster and stronger baseline for vision language model. *arXiv preprint arXiv:2402.03766*, 2024. [2](#)
- [10] Alexey Dosovitskiy, German Ros, Felipe Codevilla, Antonio Lopez, and Vladlen Koltun. Carla: An open urban driving simulator. In *Conference on robot learning*, pages 1–16. PMLR, 2017. [1](#)
- [11] Haoyu Fu, Diankun Zhang, Zongchuang Zhao, Jianfeng Cui, Dingkang Liang, Chong Zhang, Dingyuan Zhang, Hongwei Xie, Bing Wang, and Xiang Bai. Orion: A holistic end-to-end autonomous driving framework by vision-language instructed action generation. *arXiv preprint arXiv:2503.19755*, 2025. [3](#), [7](#)
- [12] Andreas Geiger, Philip Lenz, Christoph Stiller, and Raquel Urtasun. Vision meets robotics: The kitti dataset. *The international journal of robotics research*, 32(11):1231–1237, 2013. [1](#)
- [13] Daya Guo, Dejian Yang, Haowei Zhang, Junxiao Song, Ruoyu Zhang, Runxin Xu, Qihao Zhu, Shirong Ma, Peiyi Wang, Xiao Bi, et al. Deepseek-r1: Incentivizing reasoning capability in llms via reinforcement learning. *arXiv preprint arXiv:2501.12948*, 2025. [2](#), [3](#), [8](#)
- [14] Kaiming He, Xiangyu Zhang, Shaoqing Ren, and Jian Sun. Deep residual learning for image recognition. In *Proc. IEEE Conf. Comp. Vis. Patt. Recogn.*, 2016. [1](#)
- [15] Edward J Hu, Yelong Shen, Phillip Wallis, Zeyuan Allen-Zhu, Yuanzhi Li, Shean Wang, Lu Wang, Weizhu Chen, et al. Lora: Low-rank adaptation of large language models. *ICLR*, 1(2):3, 2022. [6](#)
- [16] Shengchao Hu, Li Chen, Penghao Wu, Hongyang Li, Junchi Yan, and Dacheng Tao. St-p3: End-to-end vision-based autonomous driving via spatial-temporal feature learning. In *Proc. Eur. Conf. Comp. Vis.*, pages 533–549, 2022. [6](#), [7](#)
- [17] Yihan Hu, Jiazheng Yang, Li Chen, Keyu Li, Chonghao Sima, Xizhou Zhu, Siqi Chai, Senyao Du, Tianwei Lin, Wenhui Wang, Lewei Lu, Xiaosong Jia, Qiang Liu, Jifeng Dai, Yu Qiao, and Hongyang Li. Planning-oriented autonomous driving. In *Proc. IEEE Conf. Comp. Vis. Patt. Recogn.*, pages 17853–17862, 2023. [1](#), [2](#), [7](#)

- [18] Wenxuan Huang, Bohan Jia, Zijie Zhai, Shaosheng Cao, Zheyu Ye, Fei Zhao, Zhe Xu, Yao Hu, and Shaohui Lin. Vision-r1: Incentivizing reasoning capability in multimodal large language models. *arXiv preprint arXiv:2503.06749*, 2025. 3
- [19] Zhijian Huang, Chengjian Fen, Feng Yan, Baihui Xiao, Zequn Jie, Yujie Zhong, Xiaodan Liang, and Lin Ma. Drivemm: All-in-one large multimodal model for autonomous driving. *arXiv preprint arXiv:2412.07689*, 2024. 2, 3, 7, 8
- [20] Jyh-Jing Hwang, Runsheng Xu, Hubert Lin, Wei-Chih Hung, Jingwei Ji, Kristy Choi, Di Huang, Tong He, Paul Covington, Benjamin Sapp, et al. Emma: End-to-end multimodal model for autonomous driving. *arXiv preprint arXiv:2410.23262*, 2024. 2, 7, 8
- [21] Xiaosong Jia, Penghao Wu, Li Chen, Jiangwei Xie, Conghui He, Junchi Yan, and Hongyang Li. Think twice before driving: Towards scalable decoders for end-to-end autonomous driving. In *Proc. IEEE Conf. Comp. Vis. Patt. Recogn.*, pages 21983–21994, 2023. 2
- [22] Xiaosong Jia, Junqi You, Zhiyuan Zhang, and Junchi Yan. Drivetransformer: Unified transformer for scalable end-to-end autonomous driving. *arXiv preprint arXiv:2503.07656*, 2025. 2
- [23] Bo Jiang, Shaoyu Chen, Qing Xu, Bencheng Liao, Jiajie Chen, Helong Zhou, Qian Zhang, Wenyu Liu, Chang Huang, and Xinggang Wang. Vad: Vectorized scene representation for efficient autonomous driving. In *Proc. IEEE Int. Conf. Comp. Vis.*, pages 8306–8316, 2023. 1, 7
- [24] Bo Jiang, Shaoyu Chen, Qian Zhang, Wenyu Liu, and Xinggang Wang. Alphadrive: Unleashing the power of vlms in autonomous driving via reinforcement learning and reasoning. *arXiv preprint arXiv:2503.07608*, 2025. 2
- [25] Kemou Jiang, Xuan Cai, Zhiyong Cui, Aoyong Li, Yilong Ren, Haiyang Yu, Hao Yang, Daocheng Fu, Licheng Wen, and Pinlong Cai. Koma: Knowledge-driven multi-agent framework for autonomous driving with large language models. *IEEE Transactions on Intelligent Vehicles*, 2024. 2
- [26] Bu Jin, Xinyu Liu, Yupeng Zheng, Pengfei Li, Hao Zhao, Tong Zhang, Yuhang Zheng, Guyue Zhou, and Jingjing Liu. Adapt: Action-aware driving caption transformer. In *2023 IEEE International Conference on Robotics and Automation (ICRA)*, pages 7554–7561. IEEE, 2023. 2
- [27] Bo Li, Yuanhan Zhang, Dong Guo, Renrui Zhang, Feng Li, Hao Zhang, Kaichen Zhang, Peiyuan Zhang, Yanwei Li, Ziwei Liu, and Chunyuan Li. Llava-onevision: Easy visual task transfer. *Transactions on Machine Learning Research*, 2024. 2, 8
- [28] Xin Li, Yeqi Bai, Pinlong Cai, Licheng Wen, Daocheng Fu, Bo Zhang, Xuemeng Yang, Xinyu Cai, Tao Ma, Jianfei Guo, et al. Towards knowledge-driven autonomous driving. *arXiv preprint arXiv:2312.04316*, 2023. 1
- [29] Xin Li, Yeqi Bai, Pinlong Cai, Licheng Wen, Daocheng Fu, Bo Zhang, Xuemeng Yang, Xinyu Cai, Tao Ma, Jianfei Guo, et al. Towards knowledge-driven autonomous driving. *arXiv preprint arXiv:2312.04316*, 2023. 2
- [30] Yongkang Li, Kaixin Xiong, Xiangyu Guo, Fang Li, Sixu Yan, Gangwei Xu, Lijun Zhou, Long Chen, Haiyang Sun, Bing Wang, et al. Recogdrive: A reinforced cognitive framework for end-to-end autonomous driving. *arXiv preprint arXiv:2506.08052*, 2025. 2, 3, 8
- [31] Zhiqi Li, Zhiding Yu, Shiyi Lan, Jiahua Li, Jan Kautz, Tong Lu, and Jose M Alvarez. Is ego status all you need for open-loop end-to-end autonomous driving? In *Proc. IEEE Conf. Comp. Vis. Patt. Recogn.*, pages 14864–14873, 2024. 1
- [32] Zhiqi Li, Zhiding Yu, Shiyi Lan, Jiahua Li, Jan Kautz, Tong Lu, and Jose M Alvarez. Is ego status all you need for open-loop end-to-end autonomous driving? In *Proc. IEEE Conf. Comp. Vis. Patt. Recogn.*, pages 14864–14873, 2024. 7
- [33] Bencheng Liao, Shaoyu Chen, Haoran Yin, Bo Jiang, Cheng Wang, Sixu Yan, Xinbang Zhang, Xiangyu Li, Ying Zhang, Qian Zhang, et al. Diffusiondrive: Truncated diffusion model for end-to-end autonomous driving. In *Proc. IEEE Conf. Comp. Vis. Patt. Recogn.*, pages 12037–12047, 2025. 2
- [34] Haotian Liu, Chunyuan Li, Qingyang Wu, and Yong Jae Lee. Visual instruction tuning. *Advances in neural information processing systems*, 36, 2024. 2, 6
- [35] Ze Liu, Yutong Lin, Yue Cao, Han Hu, Yixuan Wei, Zheng Zhang, Stephen Lin, and Baining Guo. Swin transformer: Hierarchical vision transformer using shifted windows. In *Proc. IEEE Int. Conf. Comp. Vis.*, pages 10012–10022, 2021. 1
- [36] Zhuang Liu, Hanzi Mao, Chao-Yuan Wu, Christoph Feichtenhofer, Trevor Darrell, and Saining Xie. A convnet for the 2020s. In *Proc. IEEE Conf. Comp. Vis. Patt. Recogn.*, pages 11976–11986, 2022. 1
- [37] Ziyu Liu, Zeyi Sun, Yuhang Zang, Xiaoyi Dong, Yuhang Cao, Haodong Duan, Dahua Lin, and Jiaqi Wang. Visual-rft: Visual reinforcement fine-tuning. *arXiv preprint arXiv:2503.01785*, 2025. 3
- [38] I Loshchilov. Decoupled weight decay regularization. *arXiv preprint arXiv:1711.05101*, 2017. 6
- [39] Jiaxing Mao, Yuxi Qian, Junjie Ye, Hang Zhao, and Yue Wang. Gpt-driver: Learning to drive with gpt. *arXiv preprint arXiv:2310.01415*, 2023. 7
- [40] Ana-Maria Marcu, Long Chen, Jan Hünermann, Alice Karnsund, Benoit Hanotte, Prajwal Chidananda, Saurabh Nair, Vijay Badrinarayanan, Alex Kendall, Jamie Shotton, et al. Lingoqa: Video question answering for autonomous driving. *arXiv preprint arXiv:2312.14115*, 2023. 2, 3, 6
- [41] Long Ouyang, Jeffrey Wu, Xu Jiang, Diogo Almeida, Carroll Wainwright, Pamela Mishkin, Chong Zhang, Sandhini Agarwal, Katarina Slama, Alex Ray, et al. Training language models to follow instructions with human feedback. *Proc. Advances in Neural Inf. Process. Syst.*, 35:27730–27744, 2022. 2
- [42] Kishore Papineni, Salim Roukos, Todd Ward, and Wei-Jing Zhu. Bleu: a method for automatic evaluation of machine translation. In *Proceedings of the 40th annual meeting of the Association for Computational Linguistics*, pages 311–318, 2002. 6
- [43] Aditya Prakash, Kashyap Chitta, and Andreas Geiger. Multi-modal fusion transformer for end-to-end autonomous driving. In *Proc. IEEE Conf. Comp. Vis. Patt. Recogn.*, pages 7077–7087, 2021. 3

- [44] Katrin Renz, Long Chen, Elahe Arani, and Oleg Sinavski. Simlingo: Vision-only closed-loop autonomous driving with language-action alignment. In *Proc. IEEE Conf. Comp. Vis. Patt. Recogn.*, pages 11993–12003, 2025. 3
- [45] John Schulman, Filip Wolski, Prafulla Dhariwal, Alec Radford, and Oleg Klimov. Proximal policy optimization algorithms. *arXiv preprint arXiv:1707.06347*, 2017. 4
- [46] Hao Shao, Yuxuan Hu, Letian Wang, Guanglu Song, Steven L Waslander, Yu Liu, and Hongsheng Li. Lmdrive: Closed-loop end-to-end driving with large language models. In *Proc. IEEE Conf. Comp. Vis. Patt. Recogn.*, pages 15120–15130, 2024. 2
- [47] Zhihong Shao, Peiyi Wang, Qihao Zhu, Runxin Xu, Junxiao Song, Xiao Bi, Haowei Zhang, Mingchuan Zhang, YK Li, Yang Wu, et al. Deepseekmath: Pushing the limits of mathematical reasoning in open language models. *arXiv preprint arXiv:2402.03300*, 2024. 2, 4
- [48] Chonghao Sima, Katrin Renz, Kashyap Chitta, Li Chen, Hanxue Zhang, Chengan Xie, Ping Luo, Andreas Geiger, and Hongyang Li. Drivelm: Driving with graph visual question answering. *arXiv preprint arXiv:2312.14150*, 2023. 2
- [49] Pei Sun, Henrik Kretzschmar, Xerxes Dotiwalla, Aurelien Chouard, Vijaysai Patnaik, Paul Tsui, James Guo, Yin Zhou, Yuning Chai, Benjamin Caine, et al. Scalability in perception for autonomous driving: Waymo open dataset. In *Proc. IEEE Conf. Comp. Vis. Patt. Recogn.*, pages 2446–2454, 2020. 1
- [50] Huajie Tan, Yuheng Ji, Xiaoshuai Hao, Xiansheng Chen, Pengwei Wang, Zhongyuan Wang, and Shanghang Zhang. Reason-rft: Reinforcement fine-tuning for visual reasoning of vision language models. In *Proc. Advances in Neural Inf. Process. Syst.*, 2025. 3
- [51] Xiaoyu Tian, Junru Gu, Bailin Li, Yicheng Liu, Chenxu Hu, Yang Wang, Kun Zhan, Peng Jia, Xianpeng Lang, and Hang Zhao. Drivevlm: The convergence of autonomous driving and large vision-language models. *arXiv preprint arXiv:2402.12289*, 2024. 2, 7
- [52] Ashish Vaswani, Noam Shazeer, Niki Parmar, Jakob Uszkoreit, Llion Jones, Aidan N Gomez, Łukasz Kaiser, and Illia Polosukhin. Attention is all you need. *Proc. Advances in Neural Inf. Process. Syst.*, 30, 2017. 1
- [53] Ramakrishna Vedantam, C Lawrence Zitnick, and Devi Parikh. Cider: Consensus-based image description evaluation. In *Proc. IEEE Conf. Comp. Vis. Patt. Recogn.*, pages 4566–4575, 2015. 6
- [54] Shihao Wang, Zhiding Yu, Xiaohui Jiang, Shiyi Lan, Min Shi, Nadine Chang, Jan Kautz, Ying Li, and Jose M Alvarez. Omnidrive: A holistic vision-language dataset for autonomous driving with counterfactual reasoning. In *Proc. IEEE Conf. Comp. Vis. Patt. Recogn.*, pages 22442–22452, 2025. 2, 3, 6, 7
- [55] Wenhui Wang, Furu Wei, Li Dong, Hangbo Bao, Nan Yang, and Ming Zhou. Minilm: Deep self-attention distillation for task-agnostic compression of pre-trained transformers. *Proc. Advances in Neural Inf. Process. Syst.*, 33:5776–5788, 2020. 5
- [56] Wenhui Wang, Jiangwei Xie, ChuanYang Hu, Haoming Zou, Jianan Fan, Wenwen Tong, Yang Wen, Silei Wu, Hanming Deng, Zhiqi Li, et al. Drivemlm: Aligning multi-modal large language models with behavioral planning states for autonomous driving. *arXiv preprint arXiv:2312.09245*, 2023. 2, 3
- [57] Weiyun Wang, Zhangwei Gao, Lixin Gu, Hengjun Pu, Long Cui, Xingguang Wei, Zhaoyang Liu, Linglin Jing, Shenglong Ye, Jie Shao, et al. Internvl3.5: Advancing open-source multimodal models in versatility, reasoning, and efficiency. *arXiv preprint arXiv:2508.18265*, 2025. 2, 8
- [58] Licheng Wen, Daocheng Fu, Xin Li, Xinyu Cai, Tao Ma, Pinlong Cai, Min Dou, Botian Shi, Liang He, and Yu Qiao. Dilu: A knowledge-driven approach to autonomous driving with large language models. *arXiv preprint arXiv:2309.16292*, 2023. 3
- [59] Xinshuo Weng, Boris Ivanovic, Yan Wang, Yue Wang, and Marco Pavone. Para-drive: Parallelized architecture for real-time autonomous driving. In *Proc. IEEE Conf. Comp. Vis. Patt. Recogn.*, pages 15449–15458, 2024. 1, 2
- [60] Julian Wörmann, Daniel Bogdoll, Christian Brunner, Etienne Bührle, Han Chen, Evaristus Fuh Chuo, Kostadin Cvejoski, Ludger van Elst, Philip Gottschall, Stefan Griesche, et al. Knowledge augmented machine learning with applications in autonomous driving: A survey. *arXiv preprint arXiv:2205.04712*, 2022. 2
- [61] Zhenhua Xu, Yujia Zhang, Enze Xie, Zhen Zhao, Yong Guo, Kwan-Yee K Wong, Zhenguo Li, and Hengshuang Zhao. Drivegpt4: Interpretable end-to-end autonomous driving via large language model. *IEEE Robotics and Automation Letters*, 2024. 2
- [62] An Yang, Baosong Yang, Binyuan Hui, Bo Zheng, Bowen Yu, Chang Zhou, Chengpeng Li, Chengyuan Li, Dayiheng Liu, Fei Huang, Guanting Dong, Haoran Wei, Huan Lin, Jialong Tang, Jialin Wang, Jian Yang, Jianhong Tu, Jianwei Zhang, Jianxin Ma, Jin Xu, Jingren Zhou, Jinze Bai, Jinzheng He, Junyang Lin, Kai Dang, Keming Lu, Keqin Chen, Kexin Yang, Mei Li, Mingfeng Xue, Na Ni, Pei Zhang, Peng Wang, Ru Peng, Rui Men, Ruize Gao, Runji Lin, Shijie Wang, Shuai Bai, Sinan Tan, Tianhang Zhu, Tianhao Li, Tianyu Liu, Wenbin Ge, Xiaodong Deng, Xiaohuan Zhou, Xingzhang Ren, Xinyu Zhang, Xipin Wei, Xuancheng Ren, Yang Fan, Yang Yao, Yichang Zhang, Yu Wan, Yunfei Chu, Yuqiong Liu, Zeyu Cui, Zhenru Zhang, and Zhihao Fan. Qwen2 technical report. *arXiv preprint arXiv:2407.10671*, 2024. 2
- [63] An Yang, Anfeng Li, Baosong Yang, Beichen Zhang, Binyuan Hui, Bo Zheng, Bowen Yu, Chang Gao, Chengen Huang, Chenxu Lv, Chujie Zheng, Dayiheng Liu, Fan Zhou, Fei Huang, Feng Hu, Hao Ge, Haoran Wei, Huan Lin, Jialong Tang, Jian Yang, Jianhong Tu, Jianwei Zhang, Jianxin Yang, Jiaxi Yang, Jing Zhou, Jingren Zhou, Junyang Lin, Kai Dang, Keqin Bao, Kexin Yang, Le Yu, Lianghao Deng, Mei Li, Mingfeng Xue, Mingze Li, Pei Zhang, Peng Wang, Qin Zhu, Rui Men, Ruize Gao, Shixuan Liu, Shuang Luo, Tianhao Li, Tianyi Tang, Wenbiao Yin, Xingzhang Ren, Xinyu Wang, Xinyu Zhang, Xuancheng Ren, Yang Fan, Yang Su, Yichang Zhang, Yinger Zhang, Yu Wan, Yuqiong Liu, Zekun Wang, Zeyu Cui, Zhenru Zhang, Zhipeng Zhou, and Zihan Qiu. Qwen3 technical report. *arXiv preprint arXiv:2505.09388*, 2025. 2, 4

- [64] An Yang, Anfeng Li, Baosong Yang, Beichen Zhang, Binyuan Hui, Bo Zheng, Bowen Yu, Chang Gao, Chengen Huang, Chenxu Lv, et al. Qwen3 technical report. *arXiv preprint arXiv:2505.09388*, 2025. 2, 3, 5, 8
- [65] Senqiao Yang, Junyi Li, Xin Lai, Bei Yu, Hengshuang Zhao, and Jiaya Jia. Visionthink: Smart and efficient vision language model via reinforcement learning. *arXiv preprint arXiv:2507.13348*, 2025. 3
- [66] Jianhao Yuan, Shuyang Sun, Daniel Omeiza, Bo Zhao, Paul Newman, Lars Kunze, and Matthew Gadd. Rag-driver: Generalisable driving explanations with retrieval-augmented in-context learning in multi-modal large language model. *arXiv preprint arXiv:2402.10828*, 2024. 2
- [67] Songyan Zhang, Wenhui Huang, Zihui Gao, Hao Chen, and Chen Lv. Wisead: Knowledge augmented end-to-end autonomous driving with vision-language model. *arXiv preprint arXiv:2412.09951*, 2024. 2, 8
- [68] Yuze Zhao, Jintao Huang, Jinghan Hu, Xingjun Wang, Yunlin Mao, Daoze Zhang, Zeyinzi Jiang, Zhikai Wu, Baole Ai, Ang Wang, Wenmeng Zhou, and Yingda Chen. Swift:a scalable lightweight infrastructure for fine-tuning, 2024. 5
- [69] Xingcheng Zhou, Xuyuan Han, Feng Yang, Yunpu Ma, and Alois C Knoll. Opendrivevla: Towards end-to-end autonomous driving with large vision language action model. *arXiv preprint arXiv:2503.23463*, 2025. 3, 7
- [70] Yunsong Zhou, Linyan Huang, Qingwen Bu, Jia Zeng, Tianyu Li, Hang Qiu, Hongzi Zhu, Minyi Guo, Yu Qiao, and Hongyang Li. Embodied understanding of driving scenarios. *arXiv preprint arXiv:2403.04593*, 2024. 2, 6
- [71] Zhiyuan Zhou, Heye Huang, Boqi Li, Shiyue Zhao, Yao Mu, and Jianqiang Wang. Safedrive: Knowledge-and data-driven risk-sensitive decision-making for autonomous vehicles with large language models. *arXiv preprint arXiv:2412.13238*, 2024. 3
- [72] Zewei Zhou, Tianhui Cai, Seth Z Zhao, Yun Zhang, Zhiyu Huang, Bolei Zhou, and Jiaqi Ma. Autovla: A vision-language-action model for end-to-end autonomous driving with adaptive reasoning and reinforcement fine-tuning. *arXiv preprint arXiv:2506.13757*, 2025. 2, 3, 6, 7

OpenREAD: Reinforced Open-Ended Reasoning for End-to-End Autonomous Driving with LLM-as-Critic

Supplementary Material

6. Visualization on the Trajectory Planning

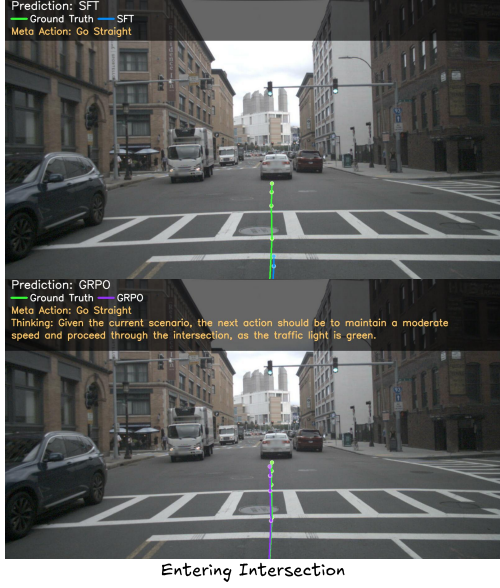


Figure 5. OpenREAD performs a less-conservative planning when entering the intersection.



Figure 6. OpenREAD performs a safe and consistent following on the wet road.

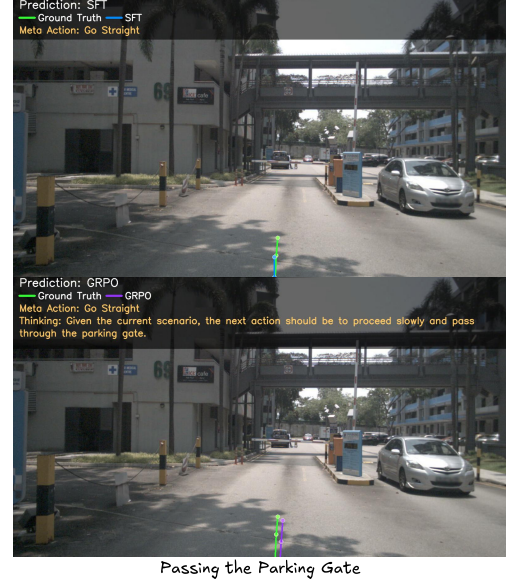


Figure 7. OpenREAD is capable of recognizing the parking gate with cautious planning.

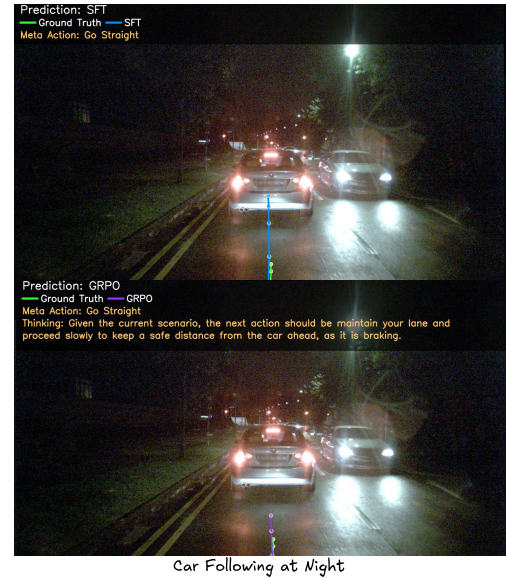


Figure 8. OpenREAD plans a slow trajectory to avoid collision with the front car at night.

7. Visualization on the Open-Ended Knowledge



Q: Is there any obstacle hindering your forward movement?

GT: The bus ahead of me.

Qwen3-VL-8B: Based on the provided images, there is no physical obstacle hindering your forward movement.\n\nThe vehicle from which the photo is taken appears to be stopped or moving very slowly in traffic. The primary impediment is not an obstacle, but rather the traffic ahead.\n\nSpecifically, you are stopped behind:\n- A red single-decker bus with the number **393** directly in front of you.\n- A red double-decker bus with the number **21** on the left, which is in a dedicated bus lane.\n\nThe road ahead is clear of any debris, barriers, or other physical impediments. The traffic lights are green, indicating that traffic should be able to proceed, although the buses are stationary, likely due to traffic flow or a stop.\n\nTherefore, while you are stopped in traffic, there is no actual obstacle blocking your path.

WiseAD: No, there are no obstacles hindering my forward movement

OpenREAD(Ours): <think>There is a bus ahead in the same lane, which is stationary or moving slowly, and it is positioned in the path of the vehicle. This bus is the only obstacle currently visible on the road that could hinder forward movement. No other vehicles, pedestrians, or road obstacles are present in the lane ahead.</think> <answer> Yes, there is an obstacle hindering my forward movement, which is the bus ahead. </answer>



Q: Why are you accelerating?

GT: Because the van ahead is pulling away

Qwen3-VL-8B: Based on the sequence of images, I am accelerating because the vehicle directly in front of me, a white van, has come to a stop at a traffic light.
Here's the reasoning:
1. **Initial State (Image 1):** The white van is driving ahead, and the road ahead is clear. I am following it at a steady speed.
2. **Stopping (Image 2 & 3):** The white van slows down and comes to a complete stop. In Image 3, a "20" speed limit sign is visible on the road, indicating a speed limit zone. The van is stopped at the stop line, which is standard behavior for a traffic light.
3. **Acceleration (Image 4 & 5):** The white van remains stopped. In Image 4, a dark blue van is now visible in the lane to my right, also stopped. In Image 5, a motorcycle is approaching from the right, and the white van is still stationary. Since the van is not moving, and the traffic light is likely red (implied by the stop), I am accelerating to pass it and continue driving.
Therefore, I am accelerating because the vehicle in front of me has stopped, and I am following the rules of the road by waiting for the light to change before proceeding.

Wise4D: I should not accelerate.

OpenREAD(Ours): **<think>**There is a visible gap in the traffic ahead, with the truck ahead moving forward and no vehicles or obstacles blocking the road. The road signs and markings indicate that it is safe to accelerate and merge into the flow of traffic. Accelerating helps maintain a safe and efficient speed on the road.**</think>** **<answer>**I am accelerating because there is a safe gap in the traffic ahead.**</answer>**



Q: What is your current driving action and it's justification?

GT: Drive slightly accelerate straight, the lights are green and there is enough space between us and the lead vehicle.

Qwen3-VL-8B: Based on the sequence of images, your current driving action is to **proceed straight through the intersection**.
Here is the justification:
1. **Traffic Light Status:** In the final image, the traffic light for your direction of travel (straight ahead) is clearly green. The light is illuminated, indicating that you have the right-of-way to proceed.
2. **Road Markings:** The road ahead is marked with a large white arrow pointing straight ahead, reinforcing the permitted direction of travel.
3. **Vehicle Position:** You are positioned in the correct lane for going straight, and the red double-decker bus in front of you is also in the same lane, moving forward. This indicates that traffic flow is normal and you are following the flow of traffic.
4. **Pedestrian and Cyclist Activity:** Pedestrians are visible on the sidewalks, and a cyclist is on the left, but they are not in your path. The traffic light for pedestrians is red, meaning they are not crossing the road, and the cyclist is on the left side of the road, not in your lane.
Therefore, the safest and most appropriate action is to continue driving straight through the intersection.

Wise4D: I am following the lane and maintaining left to be correctly centered in the lane and to keep a safe distance from the adjacent lane on the right.

OpenREAD(Ours): <think>The traffic lights ahead are green, indicating that vehicles are permitted to proceed through the intersection. There are no visible road signs or signals requiring a stop or change in direction. Since the traffic light is green and the road ahead is clear, the appropriate action is to continue driving forward.</think> <answer>My current driving action is to accelerate because the traffic lights are green.</answer>